MODELING OF ICE-STORAGE TANKS

T.B. Jekel
Student Member ASHRAE

J.W. Mitchell, Ph.D.
Member ASHRAE

S.A. Klein, Ph.D.
Member ASHRAE

ABSTRACT

A mechanistic model has been developed for static ice-storage tanks for both charging and discharging periods. This paper describes the basic heat transfer analysis and presents the characteristics of the charging and discharging periods determined from the model. An effectiveness approach is developed to describe the tank operation and is used to validate the model with manufacturer's data. The tank effectiveness is generated for both charging and discharging as a function of control variables. The effectiveness concept allows a computationally efficient prediction of the time-dependent performance of an ice-storage tank to be made. The effectiveness approach also provides a format for correlation of experimental data and manufacturers' information.

INTRODUCTION

The use of ice-storage systems for air-conditioning applications is increasing due to the need to reduce peak power requirements resulting from air conditioning. Many utility companies offer variable rate structures that encourage energy use during off-peak periods. Ice-storage systems are able to take advantage of these rate structures.

There are several possible configurations for an ice tank and chiller. The series configuration with the chiller upstream, shown in Figure 1, is common with ice-on-coil systems. Chilled water leaving the chiller passes through a large number of small tubes in the tank that effectively transfer the heat from the storage medium (ice/water) to the transport fluid (brine) and provide a large surface area per unit of storage. During the charging period, cold brine is circulated through the tubes and ice builds up on the outside of the tubes. During the discharging period, relatively warm brine is circulated through the same tubes and ice is melted around the tubes. The changes in thickness of the layer of ice on the outside of the tubes change the thermal resistances. The performance of the tank is thus a function of the current storage capacity and, consequently, time.

There is a power saving possible by operating the chiller at a relatively high discharge temperature and utilizing the low temperature of the ice tank to bring the brine temperature down to the desired blended outlet temperature. In typical operation, the flow through the tank would be controlled to produce the desired temperature entering the coil. The flow through the tank thus changes with time, and the inlet temperature also may change as the chiller load changes. Models of tank operation need to accommodate these changes in flow and inlet temperature.

In this paper, a mechanistic model is developed to simulate the time-dependent performance of a static ice-on-coil ice-storage tank. Basic heat transfer and thermodynamic relations are employed to solve for the rate of heat transfer from the brine to the tank during both charging and discharging. The performance from the model compares favorably with manufacturers' data. A heat exchanger effectiveness approach is then developed based on the simulation results for charging and discharging. The effectiveness concept is useful for design, for simulation of performance, and for correlating manufacturers' data.

ANALYSIS

The model is based on a mechanistic analysis of the melting and freezing of water around the coils. The governing equations are derived from an energy balance on the tank and heat transfer rate equations. An energy balance on the water and ice in a constant-pressure tank is

$$\dot{Q}_b + \dot{Q}_{gain} = \frac{dH}{dt} = m\frac{\partial h}{\partial t} + h\frac{\partial m}{\partial t} \qquad (1)$$

The heat transfer rate from the brine to the ice, $\dot{Q}_b$, is given by

$$\dot{Q}_b = \dot{m}_b\, c_b\, (T_{b,in} - T_{b,out}) \qquad (2)$$

The heat transfer rate from the ambient to the ice in the tank is given by

$$\dot{Q}_{gain} = UA_{amb}\, (T_{amb} - T_{tank}) \qquad (3)$$

The rate of change of the enthalpy of the storage media can be written as the sum of latent and sensible changes in the ice and the sensible change in the water:

$$\dot{Q}_b + \dot{Q}_{gain} = -h_{if}\frac{dm_{ice}}{dt} + m_{ice}\, c_{ice}\frac{dT_{ice}}{dt} + m_w\, c_w\frac{dT_w}{dt} \qquad (4)$$

Todd B. Jekel is a research assistant in the Solar Energy Laboratory and **John W. Mitchell** and **Sanford A. Klein** are professors of mechanical engineering at the University of Wisconsin, Madison.

The brine temperature changes with flow length. The relation between the brine temperature and the heat transfer to the storage media is given by an energy balance of the form

$$\dot{m}_b\, c_b \frac{dT_b}{dx} = \dot{q}_b \tag{5}$$

The heat transfer rate per unit length between the storage media and the brine is represented by a steady-state relation of the form

$$\dot{q}_b = UA'_t\,(T_s - T_b), \tag{6}$$

where A'_t is the area per unit length based on the outside diameter of the tubes and T_s is the temperature of the storage media. The specific temperature to be used in Equation 6 depends on whether the tank is charging or discharging and will be discussed later.

The overall conductance between the brine and the storage media is given in terms of the component thermal conductances as

$$UA_t = \left[\frac{1}{A_i\, h_b} + \frac{1}{UA_{storage}}\right]^{-1}, \tag{7}$$

where the first term is the convective resistance between the brine and tube wall. The second term represents the thermal conductance of the tube and the ice-water layer. The evaluation of this thermal conductance depends on whether the tank is being charged or discharged, and specific relations are developed in the appropriate sections.

A key assumption in the analysis is that the conductance, UA'_t, is constant with length along the tube. In reality, the conductance through the ice-water layer varies as the thickness varies. For example, during discharge, the ice layers are thinner near the warm brine inlet and thicker near the discharge. The assumption

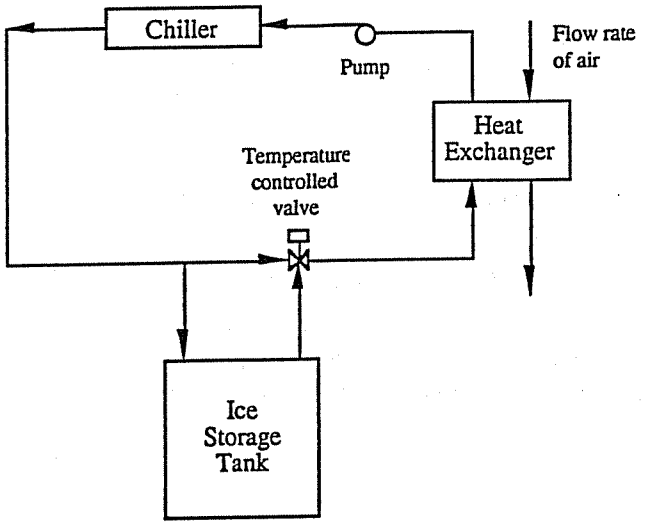

Figure 1 Series configuration of chiller and ice tank with the chiller upstream.

that the conductance is constant allows Equation 5 to be integrated analytically to yield the brine temperature at any position. The resulting relation is

$$T_b = T_s + (T_{b,in} - T_s)\, exp\left(\frac{-\,UA_t\, x}{\dot{m}_b\, c_b\, L}\right). \tag{8}$$

The log-mean-temperature difference is defined from Equation 8 as

$$\Delta T_{lm} = \frac{(T_{b,out} - T_s) - (T_{b,in} - T_s)}{\ln\left((T_{b,in} - T_s)/(T_{b,out} - T_s)\right)}. \tag{9}$$

Utilizing ΔT_{lm}, the heat transfer rate between the brine and the ice is given in terms of the log-mean-temperature-difference as

$$\dot{Q}_b = UA_t\, \Delta T_{lm}. \tag{10}$$

The heat transfer from the brine to the storage at any time is represented by Equation 10. An alternate representation is that of the thermal effectiveness (London and Kays 1964), which is useful for describing the performance of conventional heat exchangers. For a heat exchanger, the effectiveness is defined as the ratio of the actual heat transfer rate to the maximum possible heat transfer rate. For both the charging and discharging periods of an ice-storage tank, the maximum possible heat transfer rate is obtained when the outlet brine temperature from the tank is equal to the phase-change temperature, T_f (32°F for water). Therefore, the effectiveness for a storage tank is defined as

$$\varepsilon = \frac{\dot{m}_b\, c_b\, (T_{b,in} - T_{b,\,out})}{(\dot{m}c)_{\text{minimum}}\, (T_{b,in} - T_f)}. \tag{11}$$

The minimum flow-rate-specific heat product for an ice-storage tank is that of the brine. Thus, Equation 11 can be simplified by canceling the mass flow rate and specific heat terms. The actual heat transfer rate during charging or discharging can be written in terms of the effectiveness,

$$\dot{Q}_b = \varepsilon\, \dot{m}_b\, c_b\, (T_{b,in} - T_f). \tag{12}$$

The overall conductance depends on the individual conductances from brine to the ice. The conductances between the outside of the tube wall and the storage media depend on whether the tank is charging or discharging and will be developed in the appropriate sections. The convective coefficient inside the tube, h_b, depends only on the brine flow rate and is determined using conventional relations for flow inside tubes. For turbulent flow (Re > 2000), the Dittus-Boelter (Incropera and DeWitt 1985) correlation for turbulent flow in a circular tube is used:

$$\overline{Nu}_D = 0.023\, Re_D^{4/5}\, Pr^{4/10}. \tag{13}$$

The laminar Nusselt number was determined using a relation for constant wall temperature that takes into account developing thermal and hydrodynamic boundary layers (Duffie and Beckman 1980):

$$\overline{Nu}_D = 3.66 + \frac{0.0534\,(Re_D\,Pr\,D/L)^{1.15}}{1 + 0.0316\,(Re_D\,Pr\,D/L)^{0.84}} \quad (14)$$

The conductance for the tube wall is based on one-dimensional conduction and is given by

$$UA_{tube} = \frac{2\,\pi\,k_{tube}\,L}{\ln D_o/D_i} \quad (15)$$

The evaluation of the conductance between the outside of the tube and the storage media depends on the thermal conditions. The analysis of heat transfer during melting and freezing of the ice is based on a horizontal, spirally wound tube with water and/or ice on the outside, with tubes spaced on a square grid as shown in Figure 2. Figure 2a shows the formation of ice on one tube, and Figure 2b shows the interaction of ice cylinders on an array of tubes during charging. The above set of equations applies to both the charging and discharging periods of tank operation. The tube-to-storage conductances will be developed in the appropriate sections pertaining to the specific mode of tank operation.

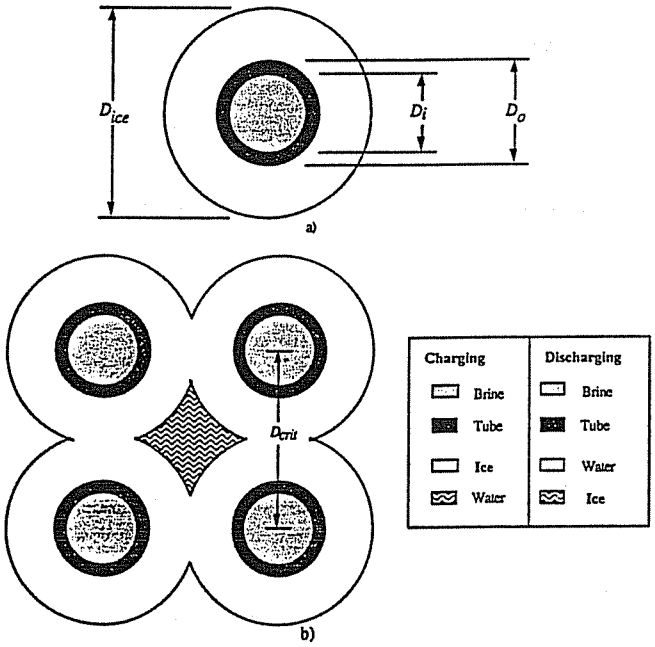

Figure 2 *a) Tube geometry and nomenclature. b) Grid geometry and nomenclature.*

HEAT TRANSFER DURING THE CHARGING PERIOD

The charging analysis is split into three periods: sensible charging, unconstrained latent charging, and constrained latent charging. Sensible charging is the process of reducing the tank water temperature to the freezing point without any phase change and occurs after the tank is completely discharged such that only water is in the tank. The unconstrained latent charging is the period when ice freezes on the tubes, but the ice formations on adjacent tubes do not intersect (Figure 2a). It is assumed that the ice freezes as cylinders around the tubes. Once the formations touch, the outside surface area of the ice that is available for heat transfer is constrained, thus the name "constrained latent charging" (Figure 2b).

During the sensible charging period, the temperature of the water is lowered to the freezing temperature. It is assumed that the tank is completely discharged and that the water in the tank is all at the same temperature. Since there is no ice building in this period, the energy balance, Equation 4, simplifies to

$$\dot{Q}_b + \dot{Q}_{gain} = m_w\,c_w\,\frac{dT_w}{dt} \quad (16)$$

The overall conductance between the brine and the water includes the convective conductances between brine and tube wall, the conductances of the tube wall, and the convective conductance on the outside the tube. The conductance is then

$$UA_t = \left[\frac{1}{A_i\,h_b} + \frac{\ln (D_o/D_i)}{2\,\pi\,k_{tube}\,L} + \frac{1}{h_w\,A_o}\right]^{-1} \quad (17)$$

The heat transfer coefficient for the water on the outside of the tube, h_w, was determined using the Churchill and Chu (Incropera and DeWitt 1985) correlation for free convection from a long, horizontal tube. The Rayleigh number uses the bulk thermal compressibility of water, which is a function of the average water temperature, with the result that the heat transfer coefficient will be lowest for the maximum water density. The mean Nusselt number based on the outside diameter of the tube is given by

$$\overline{Nu}_D = \left(0.60 + \frac{0.387\,Ra_D^{1/6}}{[1 + (0.559/Pr)^{9/16}]^{8/27}}\right)^2 \quad (18)$$

During the unconstrained latent charging period, the charging rate is affected by the amount of ice on the tubes. In order to simulate the transient response of the ice tank, Equation 4 must be solved to determine the new ice thickness. It was established that due to the small temperature difference between the ice and the working fluid, the sensible energy changes of the water and the ice are small relative to the energy involved in the phase change. For the ice tank discussed later, the sensible capacity of the ice is less than 4% of the latent capacity for a 20°F subcooling of the water. In addition, since ice does not build on the tubes until the average water temperature is at the freezing point, the sensible energy change of the water is essentially zero when

freezing initiates. Neglecting the sensible terms allows the energy balance to be written as

$$\dot{Q}_b + \dot{Q}_{gain} = - h_i f \frac{dm_{ice}}{dt} . \quad (19)$$

The overall conductance between the brine and the storage medium, based on the outside area of the ice, now includes the thermal conductance of the ice that is formed on the tubes. The heat transfer is assumed to be one-dimensional in cylindrical coordinates. The conductance is

$$UA_t = \left[\frac{1}{A_i h_b} + \frac{\ln (D_o/D_i)}{2 \pi k_{tube} L} + \frac{\ln (D_{ice}/D_o)}{2 \pi k_{ice} L} + \frac{1}{h_w A_{ice}} \right]^{-1} , \quad (20)$$

where the area of the ice is

$$A_{ice} = \pi D_{ice} L . \quad (21)$$

The heat transfer coefficient on the outside of the ice cylinder uses the same correlations as in the sensible charging period. The temperature, T_s, for the unconstrained latent charging period is the average temperature of the water, which is assumed to be constant at 32°F. The ice diameter is determined by solving Equation 19 for the differential change in mass of ice, integrating the change in mass over time and then computing the diameter from the mass.

The constrained latent charging period starts when the ice cylinders touch. At this point, the diameter equals one-half the tube spacing and is termed the critical diameter. During the constrained latent charging period, the heat transfer is no longer one-dimensional and the boundary conditions preclude an analytical solution. Cummings (1989) performed a numerical analysis to determine the thermal resistance for a specific geometry. His results will be extended to a broader range of geometries.

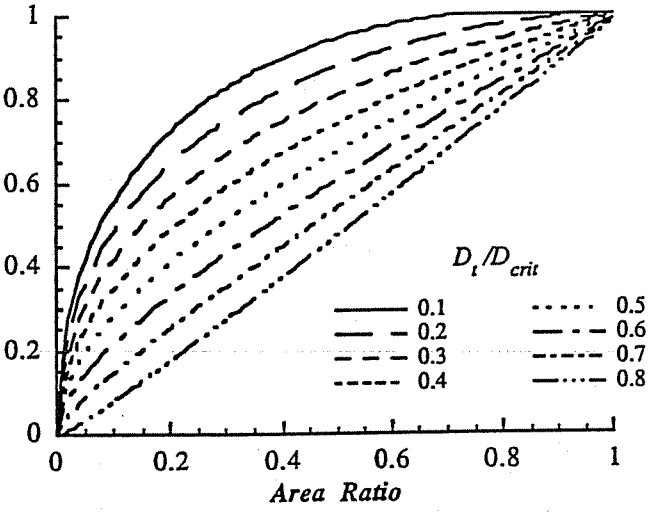

Figure 3 *Correction factor, f, as a function of the area ratio and the ratio of the outside tube diameter to the critical diameter.*

A finite-element heat transfer program, FEHT (Klein et al. 1991), was used to numerically determine the thermal conductance for a range of ratios of tube diameter to tube spacing from 0.1 to 0.8. From the results of the finite-element analysis a correction factor, f, was developed to correct the analytical expression for one-dimensional heat transfer through the ice cylinder when the ice cylinders just touch. The factor is defined from

$$\dot{Q}_{act} = f \dot{Q}_{crit} = f \frac{2 \pi k_{ice} L}{\ln (D_{crit}/D_o)} , \quad (22)$$

where $\dot{Q}_{act}$ is determined from the two-dimensional finite-element analysis. A graph of the resulting correction factors as a function of area ratio is shown in Figure 3. The correction factor, f, is a function only of geometric quantities and was correlated with nondimensional geometric variables to obtain the following relation:

$$f = -1.441\, AR + 2.455 \sqrt{AR} + \frac{D_o}{D_{crit}} (3.116\, AR - 3.158 \sqrt{AR}) \quad (23)$$

where the area ratio is AR, the ratio of the actual heat transfer area to the area that would be available if the area were not constrained, and is given by

$$AR = 1 - \frac{4}{\pi} \cos^{-1} \left(\frac{D_{crit}}{D_{ice}} \right) . \quad (24)$$

The correction factor is then used to modify the conductance of the ice. The overall conductance is given by

$$UA_t = \left[\frac{1}{A_i h_b} + \frac{\ln (D_o/D_i)}{2 \pi k_{tube} L} + \frac{\ln (D_{crit}/D_o)}{2 \pi k_{ice} L f} + \frac{1}{h_w A_{ice}} \right]^{-1} . \quad (25)$$

The heat transfer coefficient between the ice surface and the water, h_w, is assumed to be constant at the value it has before the water formations intersect.

HEAT TRANSFER DURING THE DISCHARGING PERIOD

The analysis of the discharge period will be split into two periods: (1) unconstrained latent discharging and (2) constrained latent and sensible discharging. The unconstrained latent discharging is characterized by the cylindrical melting of ice around the tubes. The constrained latent and sensible discharging is characterized by the melting of ice after the advancing water formations intersect and by the sensible discharging of the water around the tubes. It is assumed that the tank is fully charged.

As in the charging model, the discharging model assumes that the tube is long and horizontal with forced convection on the inside of the tube. On the outside of the tubes, conductive heat transfer occurs through the water before adjacent formations intersect. It is assumed that there is no convection due to the small density gradients and constrained area around the tubes.

The unconstrained latent discharging period is characterized by a cylindrical melting of ice around the outside of the tubes. The picture is similar to that for freezing, as shown in Figure 2b. The sensible internal energy change in the ice is small since the ice is assumed to melt at constant temperature. However, the sensible internal energy change in the water can be significant. Equation 4 can be simplified to

$$\dot{Q}_b + \dot{Q}_{gain} = h_{if}\frac{dm_w}{dt} + m_w\, c_w \frac{dT_w}{dt}, \qquad (26)$$

where dm_w/dt is the rate of change of the mass of water.

When the discharge period starts, there is no water around the tubes. It is assumed that the temperature on the outside of the tube is at the freezing point and the temperature of the surface of the ice is constant at the freezing point. The total conductance between the brine and the surface of the tube is given by

$$UA_t = \left[\frac{1}{A_i\, h_b} + \frac{ln\,(D_o/D_i)}{2\,\pi\, k_{tube}\, L} + \frac{ln\,(D_w/D_o)}{2\,\pi\, k_w\, L}\right]^{-1}. \qquad (27)$$

The value of the storage media temperature to be used with this conductance-area product, T_s in Equation 6, is the temperature of the ice boundary and is assumed to be 32°F during discharge.

After the water formations intersect, the heat transfer occurs from the brine to the water and then from the water to the ice. Heat transfer coefficients between the tube and the water and between the water and the ice for this geometry are not known. It is assumed that the overall conductance-area product between the tube and the water when the water formations intersect remains constant during the rest of the discharging period.

RESULTS AND VALIDATION

The latent charging rate as a function of the percent of latent capacity was determined from the model and is shown in Figure 4 for several inlet brine temperatures. During the unconstrained latent charging period, the charging rate is nearly constant, but it drops significantly in the constrained latent charging period. The breaks in the curves correspond to the points at which the adjacent ice formations touch. The charging rate decreases with increasing brine inlet temperature.

The performance predicted by the model was compared with performance data available from one manufaturer (CMC 1987). The working fluid is 25% ethylene glycol, and the nominal capacity of the ice-storage tank is 190 ton-hours, which includes the latent capacity of the ice and sensible capacity of the water heated to a temperature of approximately 60°F. The manufacturer does not provide data for charging rate as a function of either state of charge or time but only average values over the entire charging period. Therefore, the validation is based on an average charging rate over the entire latent charging period, which does not provide a detailed comparison.

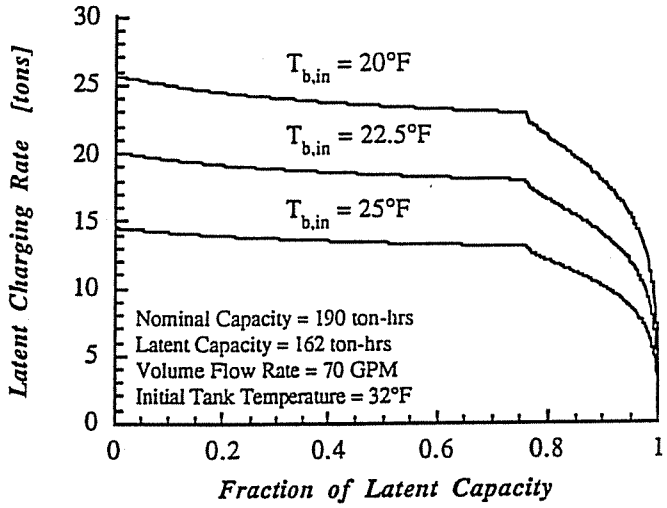

Figure 4 Charging rate for several inlet brine temperatures as a function of latent capacity.

The average charging rates given by the model were found to be always somewhat less than the data. For a given inlet brine temperature and volume flow rate, the average charging rate is 12% low on the average. However, for a given charging rate and volume flow rate, the inlet brine temperature was within 2°F of the manufacturer's stated inlet brine temperature. Since the charging rate is very sensitive to the inlet brine temperature, a major reason for the discrepancy was the assumption of a constant inlet brine temperature in the model predictions.

The discharge rate for constant flow through the tank and inlet temperature is shown in Figure 5 as a

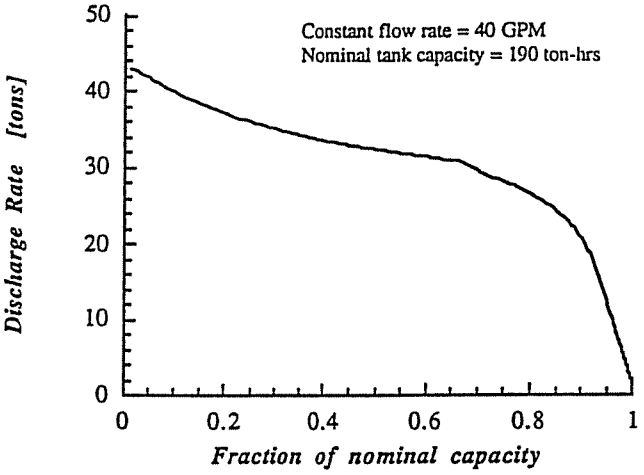

Figure 5 Discharging rate as a function of nominal capacity.

function of state of change. The discharge rate decreases as the ice around the tube melts, and it drops sharply when formations touch. The manufacturer publishes the discharging rate of the tank as a function of the inlet brine temperature, the desired blended outlet temperature, and the fraction of nominal storage capacity. The model predicts results for high outlet temperatures and low discharge rates accurately. However, when the discharge rate is high, the model usually underpredicts the fraction at which the tank could no longer meet the load compared to data. When the outlet temperature is low, the model usually overpredicts the fraction at which the tank could no longer meet the load. In addition, the model overpredicts tank performance near the end of the unconstrained discharge period (i.e., storage fractions between 0.5 and 0.65).The fraction of nominal capacity at which the ice-storage tank could no longer meet the given load was 10% different from the predicted fraction on the average.

During discharge, the heat transfer coefficient of the brine is indeterminant because the Reynolds number of the flow through the tubes is in the transition range between laminar to turbulent flow. If the laminar value of the Nusselt number is used, the heat transfer rate is too low and the performance of the tank is decreased significantly below the manufacturer's experimental performance, while the turbulent relation yields too high a value. Therefore, an interpolation scheme was defined between Reynolds numbers of 700 and 1,300. Below 700 the flow was considered laminar, and above 1,300 it was considered turbulent. Between the values, the Nusselt number was assumed to vary linearly between the turbulent and laminar values.

The model was then used to determine the thermal effectiveness of the ice-storage tank as a function of the charged fraction of latent capacity for the latent charging period. The latent capacity is based on all of the water freezing and is the product of water mass and latent heat of fusion. Figure 6 shows the dependence of the effectiveness on the fraction of capacity and volume flow rate of brine through the tank for an inlet brine temperature of 25°F. The effectiveness decreases as the charged capacity and the volume flow rate of brine through the tank increase. The effectiveness was found to be nearly independent of inlet brine temperature for the unconstrained latent charging period.

For the discharge period, the effectiveness was determined as a function of the discharged capacity for constant inlet brine temperature and a constant flow rate through the tank. The maximum capacity is obtained by melting the ice and heating the water to the brine inlet temperature:

$$\text{Maximum Capacity} = m_{ice}\,(h_{if} + c_w\,(T_{b,in} - T_f)). \quad (28)$$

Figure 7 shows the dependence of the effectiveness on the discharged capacity ratio and the mass flow rate of brine through the tank for an inlet brine temperature of 60°F. The effectiveness decreases with decreasing capacity and increasing mass flow rate through the tank.

The effectiveness as a function of inlet brine temperature and discharged capacity ratio is shown in in Figures 8, 9, and 10. In Figure 8, the effectiveness curves for a flow rate of 40 gpm and three inlet temperatures of 45°F, 50°F, and 60°F are given. The effect of inlet temperature is accounted for using the effec-tiveness based on the inlet temperature as given in Equation 11 and the maximum capacity, which also includes the effect of inlet temperature. Figures 9 and 10 are for flow rates of 60 and 80 gpm, respectively, and the effectiveness again describes the performance at these conditions also.

Also shown in Figures 8, 9, and 10 are values calculated from the manufacturer's model. The manufactur-

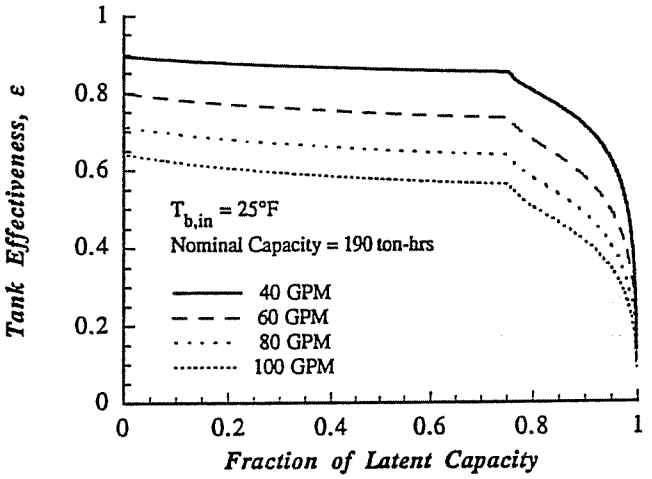

Figure 6 *Charging effectiveness as a function of latent capacity for several volume flow rates of brine through the tank.*

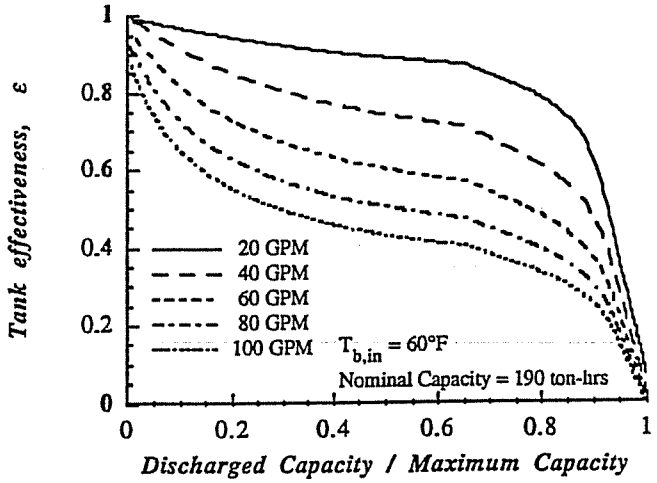

Figure 7 *Discharging effectiveness as a function of discharged capacity ratio for several flow rates through the tank.*

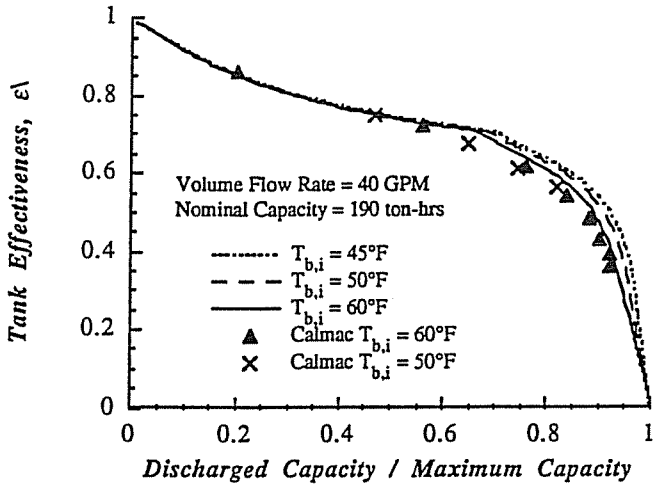

Figure 8 Discharged effectiveness as a function of discharge capacity ratio for 40 gpm.

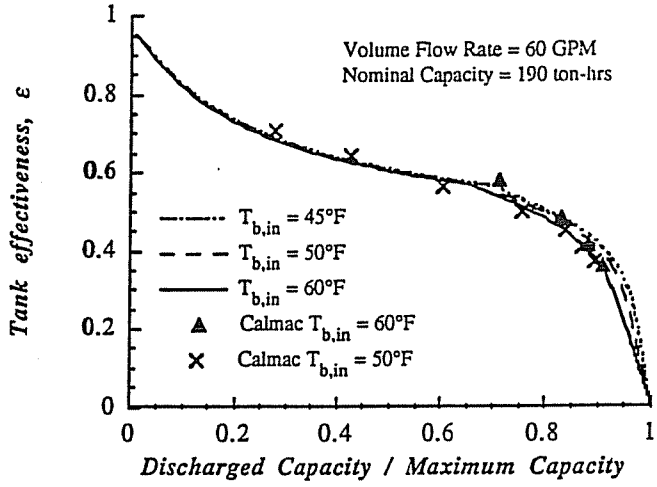

Figure 9 Discharge effectiveness as a function of discharge capacity ratio for 60 gpm.

er's results for a given flow and different temperatures also are described using the effectiveness expression. The comparison between the manufacturer's results and the model prediction further establishes the accuracy of the model.

The effectiveness concept also provides a simple model for the prediction of tank performance. For the latent charging period, the tank effectiveness at any time can be determined from the current charged fraction of latent capacity and the volume flow rate of the brine. The charging rate can be determined from the effectiveness and the inlet brine temperature. The change in charge over time can be determined by integrating the charging rate. If the volume flow rate of brine is changed during the charging period, the performance can be calculated by using the effectiveness curve for that particular flow rate.

For the discharge period, the tank effectiveness can be determined if both the initial capacity relative to the maximum and the volume flow rate of brine through the tank are known. The instantaneous discharge rate can then be determined from the effectiveness and the inlet brine temperature. Different inlet brine temperatures are described by the same effectiveness curve, while different flow rates require a different curve. The new state of charge after a period of time can then be determined by numerical integration of the discharging rate. This procedure will allow determination of the rate of discharge over time.

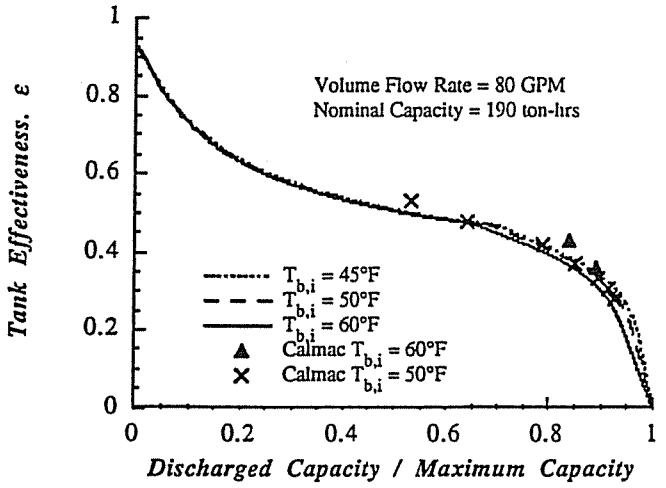

Figure 10 Discharge effectiveness as a function of discharge capacity ratio for 80 gpm.

CONCLUSIONS

The charging and discharging periods of the static ice-on-coil, ice-storage tank with brine as the working fluid were modeled based on heat transfer mechanisms. A specific tank geometry was considered, but the basic relations are applicable to other ice storage systems. The charging rates from the model were within 12% of a manufacturer's average charging data. The discharging rates from the model were within 10% of the discharging data.

The effectiveness concept for both the latent charging and the discharging of ice-storage tanks was developed. The effectiveness correlates the effect of inlet temperature. The tank charge is correlated in terms of the maximum capacity based on inlet temperature. The effectiveness provides a simple model for predicting tank performance, and is useful for correlating experimental data.

NOMENCLATURE

A = area, ft^2 (m^2)
A' = area per unit tube length, ft^2 (m^2)
AR = ratio of actual area to maximum available area after heat transfer area becomes constrained

c = constant pressure specific heat, Btu/lb·°F (kJ/kg·°C)
D = diameter, ft (m)
f = geometric correction factor for determination of constrained conductance
H = total enthalpy, Btu (kJ)
h = specific enthalpy, Btu/lb (kJ/kg)
heat transfer coefficient, Btu/h-ft^2·°F (W/m^2·C)
h_b = heat transfer coefficient between the tube and the water, Btu/h ft^2·°F (W-/m^2·C)
h_{if} = heat of fusion of ice, Btu/lb
h_w = heat transfer coefficient between the water and ice or water and tube, Btu/h·ft^2·°F (W/m^2·°C)
k = thermal conductivity, Btu/h·ft·°F (W/m·°C)
L = tube length, ft (m)
m = mass, lb (kg)
$\dot{m}$ = mass flow rate of brine, lb/h (kg/s)
Nu_D = average Nusselt number, hD/k
Pr = Prandtl number
q_b = local heat transfer rate per unit length, Btu/h·ft (W/m)
$\dot{Q}_{act}$ = total actual heat transfer rate, Btu/h (W)
$\dot{Q}_b$ = total heat transfer rate from brine to system, Btu/h (W)
$\dot{Q}_{crit}$ = total heat transfer rate when formations touch, Btu/h (W)
$\dot{Q}_{gain}$ = total heat transfer rate from the ambient to the system, Btu/h (W)
Ra_D = Rayleigh number based on diameter
Re_D = Reynolds number based on diameter
T = temperature, °F (°C)
t = time, h (s)
ΔT_{lm} = log-mean temperature difference, °F (°C)
U = conductance, Btu/h·ft^2·°F (W/m^2·°C)
UA = conductance-area product, Btu/h·°F (W/°C)
x = position along tube length, ft (m)
ε = thermal effectiveness

Subscripts

amb = ambient
b = brine
crit = critical, corresponding to where formations touch
i = inside of tubes
ice = ice
in = brine inlet
o = outside of tubes
out = brine outlet
s = surface
t = total, or overall
tube = tube
w = water
tank = tank
storage = storage media
f = phase change

REFERENCES

CMC. 1987. *Levload ice bank performance manual.* Product Literature, Calmac Model 1190. Englewood, NJ: Calmac Manufacturing Corporation.

Cummings, M.S. 1989. Modeling, design, and control of partial ice-storage air-conditioning systems. M.S. thesis, University of Wisconsin—Madison.

Duffie, J.A., and W.A. Beckman. 1980. *Solar engineering of thermal processes.* New York: John Wiley & Sons.

Incropera, F.P., and D.P. DeWitt. 1985. *Introduction to heat transfer.* New York: John Wiley & Sons.

Jekel, T.B. 1991. Modeling of ice-storage systems. M.S. thesis, University of Wisconsin—Madison.

Klein, S.A., W.A. Beckman, and G.E. Myers. 1991. *FEHT, Finite element heat transfer program.* F-Chart Software, Version 5.49. Middleton, Wisconsin.

London, A.L., and W.M. Kays. 1964. *Compact heat exchangers.* New York: McGraw Hill.